

# Strategies for High-Throughput, Templated Zeolite Synthesis

Ligang Chen and Michael W. Deem

Department of Chemical Engineering

University of California, Los Angeles, CA 90095–1592

November 20, 2018

## **Abstract**

How best to design and redesign high-throughput experiments for zeolite synthesis is addressed. A model that relates materials function to chemical composition of the zeolite and the structure directing agent is introduced. Using this model, several Monte Carlo-like design protocols are evaluated. Multi-round protocols are found to be effective, and strategies that use *a priori* information about the structure-directing libraries are found to be the best.

# 1 Introduction

Zeolites have found wide industrial applications in processes such as catalysis, molecular sieving, gas separation, and ion exchange. The significant catalytic activity and selectivity of zeolite materials are attributed to the large internal surface area and highly distributed active sites that are accessible through uniformly-sized pores. However, due to the desire to improve the quality of known zeolites that are small or faulted and the continuing quest for new zeolites with different functionalities, novel syntheses of zeolites with various frameworks and chemical compositions have drawn heavy research attention. To date, roughly 150 framework structures have been reported. New structures are added at the pace of roughly 6 per year. The use of organo-cation template molecules to provide structure direction has given rise to breakthroughs in zeolite science and provides much of the impetus for current synthetic efforts [1, 2]. The addition of organic templates such as amines and alkylammonium ions to zeolite synthesis gels can affect the rate at which a particular material is formed and can make new structures or framework chemical compositions accessible. In some cases, a strong correlation between the geometry of the structure directing organic molecule and the zeolite pore architecture is found. The nature and extent of interactions between the organic templates and the inorganic components of a zeolite synthesis gel are key parameters that determine the final zeolite pore architecture [3, 4].

We are interested in high-throughput synthesis of zeolites. High-throughput, or combinatorial, methods allow for simultaneous creation of a large number of structurally diverse and complex compounds, generalizing the traditional techniques of single compound synthesis. Monte Carlo methods have been proposed and shown to be efficient methods for

library design and re-design in both material discovery [5, 6] and small molecule design [7]. Material discovery deals with continuous variables, such as composition variables and non-composition variables. Small molecule design deals with discrete variables, such as the identities of template and ligand. For templated zeolite synthesis, we have both the continuous zeolite composition and non-composition variables and the discrete identity variables of the component parts of the organic structure-directing molecules. All of these variables affect the final zeolite material in an interrelated way.

We here propose several strategies for templated, high-throughput zeolite synthesis. In section 2 we introduce a new random energy model that serves as a surrogate for experimental measurement of the figure of merit. This random energy model is based upon models used in material discovery and small molecule design. The random energy model is not fundamental to the protocols; it is introduced as a simple way to test, parameterize, and validate the various searching methods. In an experimental implementation, the random energy model will be replaced by the value returned by the screen. In section 3, we introduce several protocols for experimentation. In section 4, we compare results of each protocol and discuss some implications. Finally, we conclude in section 5.

## 2 Random Energy Model

To test proposed protocols in an efficient fashion, we need a model in lieu of the real experimental screening process. That is, we need a model that relates the chemical composition of the zeolite and structure directing agent to the function, or figure of merit, of the material. This model is not essential to the protocols. It is simply a fast and cheap means

to test proposed protocols. This model will capture the essence of the physical system and provide validation for the protocols. Random energy models have proven useful for the study of several complex fields, including protein folding [8, 9], protein molecular evolution [10], material discovery [5], and small molecule design [7].

To consider template-assisted zeolite synthesis, we use a model that combines ideas from both material discovery [5] and small molecule design [7]. The value of the figure of merit is naturally a sum of a zeolite energy and a well-chosen organic molecular energy:

$$E = E_{\text{zeolite}} + E_{\text{molecule}} \tag{1}$$

The zeolite framework composition variables  $x_i$ ,  $d$  in number, are certainly key variables in  $E_{\text{zeolite}}$ . The composition variables are specified by the mole fractions  $x_i$ , with  $0 \leq x_i \leq 1$ , and  $\sum_{i=1}^d x_i = 1$ . Typical elemental compositions in zeolite frameworks include silicon, oxygen, aluminum, phosphorus, boron, and germanium, among others. As discussed in the Appendix, the allowed compositions are constrained to lie within a simplex in  $d - 1$  dimensions. Several phases will exist for different compositions of the material. The figure of merit will be dramatically different between each of these distinct phases. To mimic this behavior, the composition variables are grouped in the Random Phase Volume Model into phases centered around  $N_x$  points  $\mathbf{x}_\alpha$  randomly placed within the allowed composition range. The phases form a Voronoi diagram, see Figure 1. The model is defined for any number of composition variables, and the number of phase points is defined by requiring the average spacing between phase points to be  $\xi = 0.25$ . To avoid edge effects, additional points are added in a belt of width  $2\xi$  around the simplex of allowed compositions. The figure of merit

should change dramatically between composition phases. Moreover, within each phase  $\alpha$ , the figure of merit should also vary with  $\mathbf{x} - \mathbf{x}_\alpha$  due to crystallinity effects such as crystallite size, intergrowths, defects, and faulting. Non-composition variables should also affect the measured figure of merit. The non-composition variables are denoted by the  $b$  variables  $z_i$ . Without loss of generality, each variable ranges  $-1 \leq z_i \leq 1$ . How the figure of merit changes with the non-composition variables should depend on the value of the composition variables. The non-composition variables fall within  $N_z$  non-composition phases. There are a factor of 10 fewer non-composition phases than composition phases. When  $\mathbf{x}$  is in composition phase  $\alpha$  and non-composition phase  $\gamma$ , the zeolite energy is given by

$$E_{\text{zeolite}}(\mathbf{x}, \mathbf{z}) = H(\mathbf{x} - \mathbf{x}^\alpha, \{G^\alpha\}) + \frac{1}{2}H(\mathbf{z}, \{G^\gamma\}) \quad (2)$$

where  $\{G^\alpha\}$  and  $\{G^\gamma\}$  are phase-dependent random Gaussian variables with zero mean and unit variance. The  $\{G^\alpha\}$  are different in each composition phase, and the  $\{G^\gamma\}$  are different in each non-composition phase. The form of the function  $H$  is

$$H(w_1, \dots, w_n, \{G\}) = G_0 + \sigma_H \sum_{k=1}^q \sum_{\substack{i_1 + \dots + i_n = k \\ i_1, \dots, i_n \geq 0}} f_{i_1 \dots i_n; k} \xi_H^{-k} G_{i_1 \dots i_n} w_1^{i_1} \dots w_n^{i_n} \quad (3)$$

The degree of the polynomial is chosen as  $q = 6$ . The set of coefficients  $\{G\}$  includes  $G_0$  and  $G_{i_1 \dots i_n}$ . The constant symmetry factors  $f_{i_1 \dots i_n; k}$  are given by

$$f_{i_1 \dots i_n; k} = \frac{k!}{i_1! \dots i_n!} \quad (4)$$

The scale factor  $\xi_H$  is chosen so that each term in the multinomial contributes roughly the same amount in the root-mean-square sense. For the composition variables  $\xi_H = \xi/2$ , and for the non-composition variables  $\xi_H = (\langle z^6 \rangle / \langle z^2 \rangle)^{1/4} = (3/7)^{1/4}$ . The  $\sigma_H$  are chosen so that the multinomial terms contribute 40% as much as the corresponding constant, phase terms,  $G_0$  in eq 3, in the root-mean-square sense.

The organic structure-directing molecules are uniquely characterized by composition, such as the identity of the template and ligands, as shown in Figure 1. Note that *template* here denotes the framework of the structure-directing molecule, onto which ligands are attached, not the entire structure-directing molecule. For simplicity, we consider the small molecule to consist of one template and six binding ligands, each drawn from a fragment library. To quantitatively describe each template and ligand, six weakly correlated descriptors are used. Their numeric values specify the characteristics of each template or ligand.

We again use a random energy model for the molecules to account for the contributions to structure direction arising from interactions between the zeolite and template and from interactions between the zeolite and each of the ligands. In addition, synergistic effects between the ligands and template are incorporated. Consider, for example, a molecule made from template number  $m$  from the template library and ligands number  $s_1, \dots, s_6$  from the ligand library. The template is characterized by six descriptors,  $D_1^{(m)}, \dots, D_6^{(m)}$ . Similarly, each ligand is characterized by six descriptors,  $d_1^{(l_i)}, \dots, d_6^{(l_i)}$ . We denote the template contribution to binding by  $E_T$  and the ligand contributions by  $E_L$ . We denote the contribution due to synergistic ligand-ligand interactions by  $E_{LL}$  and the contribution due to synergistic template-ligand interactions by  $E_{TL}$ . The total molecular contribution to the figure of merit is, then,

$$E_{\text{molecule}} = E_{\text{L}} + E_{\text{T}} + E_{\text{LL}} + E_{\text{TL}} \quad (5)$$

Each of these terms is given in the form of a random polynomial:

$$E_{\text{L}}(\mathbf{x}, \mathbf{z}) = \sum_{i=1}^6 F[d_1^{(l_i)}, \dots, d_6^{(l_i)}, \{G_{\text{L}}(\mathbf{x}, \mathbf{z})\}], \quad G_{\text{L}}(\mathbf{x}, \mathbf{z}) = \lambda_{x,1} G_{\text{L}}^{\alpha} + \frac{1}{2} \lambda_{z,1} G_{\text{L}}^{\gamma} \quad (6)$$

$$E_{\text{T}}(\mathbf{x}, \mathbf{z}) = F[D_1^{(m)}, \dots, D_6^{(m)}, \{G_{\text{T}}(\mathbf{x}, \mathbf{z})\}], \quad G_{\text{T}}(\mathbf{x}, \mathbf{z}) = \lambda_{x,2} G_{\text{T}}^{\alpha} + \frac{1}{2} \lambda_{z,2} G_{\text{T}}^{\gamma} \quad (7)$$

$$E_{\text{LL}}(\mathbf{x}, \mathbf{z}) = \sum_{i=1}^6 h_i(\mathbf{x}, \mathbf{z}) F[d_{j_1}^{(l_i)}, d_{j_2}^{(l_i)}, d_{j_3}^{(l_i)}, d_{j_4}^{(l_{i+1})}, d_{j_5}^{(l_{i+1})}, d_{j_6}^{(l_{i+1})}, \{G_{\text{LL}}(\mathbf{x}, \mathbf{z})\}],$$

$$G_{\text{LL}}(\mathbf{x}, \mathbf{z}) = \lambda_{x,3} G_{\text{LL}}^{i,\alpha} + \frac{1}{2} \lambda_{z,3} G_{\text{LL}}^{i,\gamma} \quad (8)$$

$$E_{\text{TL}}(\mathbf{x}, \mathbf{z}) = \sum_{i=1}^6 h_i(\mathbf{x}, \mathbf{z}) F[d_{k_1}^{(l_i)}, d_{k_2}^{(l_i)}, d_{k_3}^{(l_i)}, D_{k_4}^{(m)}, D_{k_5}^{(m)}, D_{k_6}^{(m)}, \{G_{\text{TL}}(\mathbf{x}, \mathbf{z})\}],$$

$$G_{\text{TL}}(\mathbf{x}, \mathbf{z}) = \lambda_{x,4} G_{\text{TL}}^{i,\alpha} + \frac{1}{2} \lambda_{z,4} G_{\text{TL}}^{i,\gamma} \quad (9)$$

where individual descriptors from each template and ligand are given in corresponding libraries. The building block for our random energy model as a function of those descriptors is

$$F(w_1, \dots, w_n, \{G\}) = \sum_{k=0}^q \sum_{\substack{i_1 + \dots + i_n = k \\ i_1, \dots, i_n \geq 0}} f_{i_1 \dots i_n; k}^{\frac{1}{2}} \xi_F^{-k} G_{i_1 \dots i_n} w_1^{i_1} \dots w_n^{i_n} \quad (10)$$

The  $\{G\}$ , again, will be composed of a composition and a non-composition piece, as indicated in eqs 6–9. We use  $q = 6$  and  $n = 6$ . Since the values of the descriptors,  $w_i$ , will be drawn from a Gaussian random distribution of zero mean and unit variance, we set the scaling factor,  $\xi_F$ , by

$$\xi_F = \left( \frac{\langle w^q \rangle}{\langle w^2 \rangle} \right)^{\frac{1}{q-2}} = \left( \frac{q!}{(q/2)! 2^{q/2}} \right)^{\frac{1}{q-2}} \quad (11)$$

In general the polynomial coefficients,  $\{G\}$  in eq (6-9), are functions of both zeolite variables

$\mathbf{x}$  and  $\mathbf{z}$ . However, for simplicity, we assume that the coefficients are phase-dependent only. Both types of zeolite phases have a significant impact on the energy function. The variables  $\{G_L^\alpha\}, \{G_L^\gamma\}, \{G_T^\alpha\}, \{G_T^\gamma\}, \{G_{LL}^{i,\alpha}\}, \{G_{LL}^{i,\gamma}\}, \{G_{TL}^{i,\alpha}\},$  and  $\{G_{TL}^{i,\gamma}\}$  are fixed random Gaussian variables with zero mean and unit variance. These coefficients are different in each phase. The structural constant  $h_i$  indicates the strength of the interaction at structure directing site  $i$ . This interaction function depends on the zeolite variables  $\mathbf{x}$  and  $\mathbf{z}$  as

$$h_i(\mathbf{x}, \mathbf{z}) = H(\mathbf{x} - \mathbf{x}^\alpha, \{G_i^\alpha\}) + \frac{1}{2}H(\mathbf{z}, \{G_i^\gamma\}) \quad (12)$$

As before  $\{G_i^\alpha\}$  and  $\{G_i^\gamma\}$  are sets of phase-dependent fixed random Gaussian variables with zero mean and unit variance. The parameter  $\sigma_H$  is adjusted so that the multinomial terms contribute roughly the same as the constant, phase terms on average. In  $E_{LL}$ , only synergistic interactions between neighboring ligands are considered, and it is understood that  $l_7$  refers to  $l_1$  in eq 8. In principle, the polynomial in eq 8 could be a function of all 12 descriptors of both ligands. We assume, however, that important contributions come from interactions among three randomly chosen distinct descriptors of ligand  $l_i, d_{j_1}^{(l_i)}, d_{j_2}^{(l_i)}$ , and  $d_{j_3}^{(l_i)}$ , and another three randomly chosen distinct descriptors of ligand  $l_{i+1}, d_{j_4}^{(l_{i+1})}, d_{j_5}^{(l_{i+1})}$ , and  $d_{j_6}^{(l_{i+1})}$ . Similarly, we assume that template-ligand contributions come from interactions between three randomly chosen distinct descriptors of the ligand,  $d_{k_1}^{(l_i)}, d_{k_2}^{(l_i)}$ , and  $d_{k_3}^{(l_i)}$ , and another three randomly chosen distinct descriptors of the template,  $D_{k_4}^{(m)}, D_{k_5}^{(m)}$ , and  $D_{k_6}^{(m)}$ . Both  $j_i$  and  $k_i$  are descriptor indices ranging from 1 to 6. We assume that these indices depend only on the template, since the molecular details of the zeolite have been suppressed. The constants  $\lambda_{x,i}$  are adjusted so that the synergistic terms in compositional phases will



contribute on average as  $E_L : E_T : E_{LL} : E_{TL} = 1 : 1 : 2 : 1.2$ . Furthermore, we adjust the  $\lambda_{x,i}$  so that the total molecular contribution from the interaction with the compositional variables accounts for roughly 15% of the constant, compositional phase term in  $E_{zeolite}$  in the root-mean-square sense. We similarly adjust the values of  $\lambda_{z,i}$  in non-compositional phases so that the contribution from the interaction with the non-composition variables is also 15%.

Finally, we minimize the energy returned by the model. That is, we sample the figure of merit,  $E$ , by  $\exp(-\beta E)$ .

### 3 Protocols for high-throughput experimentation

As in the small molecule case [7], we first build the template and ligand libraries. We denote the size of the template library by  $N_T = 15$  and the size of the ligand library by  $N_L = 1000$ . In a real experiment, the six descriptors would then be calculated for each template and ligand. In the simulated experiment, the values of the six descriptors of each ligand and template are extracted from a Gaussian random distribution with zero mean and unit variance. In the simulated experiment, we also associate two sets of random interaction descriptor indices to each template for the interaction terms in eq 8 and 9.

For comparison, we fix the total number of samples to be synthesized at 100000 for all protocols. That is, we keep roughly the same experimental cost.

We consider several single pass protocols. Current high-throughput experiments uniformly tend to perform a single-pass, grid search on all continuous variables. To mimic current experiments, we use such a grid search on the composition and non-composition variables. For the discrete molecular variables, we instead randomly pick one template and

six ligands from the corresponding libraries. In another single-pass protocol, which we call random, we search randomly over all variables, *i.e.* we choose the composition variables and non-composition variables at random as well.

We also consider several multi-pass protocols. Unlike single-pass protocols, multi-pass protocols allow us to learn about the system as the experiment proceeds. In analogy to Monte Carlo methods, each round of combinatorial chemistry experiments corresponds to a move in a Monte Carlo simulation. Instead of tracking one system with many configurational degrees of freedom, however, many samples are tracked. This results in a rather diverse population of samples and increases the opportunity for a few zeolite samples to survive more elaborate tests for application performance, tests that are only roughly correlated with the primary screen. The existence of these secondary and primary screens is the reason why sampling the figure of merit to find several promising compounds is so important. We use a Monte Carlo protocol so as to maintain diversity in the samples. Genetic algorithms, while powerful at local optimization, reduce the diversity of the population in the cross-over step and tend to fail diversity tests [7]. To be consistent with current experiments, we prefer to synthesize 1000 samples simultaneously and perform Monte Carlo moves on every sample for 100 rounds. The initial sample configurations are assigned by the random protocol.

We change the zeolite variables as well as the components of the structure directing agent at each round of the Monte Carlo protocol. In the simplest approach, we perturb both the composition variables and the non-composition variables of the zeolite part around the original value using the traditional Metropolis-type method. For the non-composition variables,  $\mathbf{z}$ , periodic boundary conditions are used. For the composition variables,  $\mathbf{x}$ , reflecting boundary conditions are used, as discussed in the Appendix. For the molecular part, either

the template is changed with probability  $p_{\text{template}}$ , or one of the six ligands is picked randomly to change in each Monte Carlo move. The new configurations are updated according to the acceptance rule at  $\beta$ , the inverse of the protocol temperature. All the samples are sequentially updated in one Monte Carlo round. For the molecular part, either a simple Metropolis method or a biased Monte Carlo method can be incorporated. In the simple Metropolis method, the new template or ligand is selected at random with a uniform probability from the corresponding libraries. The final acceptance rule for an unbiased protocol, which is applied after the zeolite and molecular variables have been modified, is

$$\text{acc}(o \rightarrow n) = \min[1, \exp(-\beta\Delta E)] \quad (13)$$

The biased Monte Carlo schemes allow us to generate a trial configuration with a probability that depends on the potential energy of that configuration. These schemes have been proven to be highly successful in small molecule high-throughput experiment design [7], where biased energy forms are constructed from either theory or pre-experiments. In the present case, since the total molecular energy is a function of both the composition and non-composition variables, it is not feasible to construct the bias from pre-experiments. We, therefore, use the theoretical bias directly from the random energy model. For a zeolite at compositional phase  $\alpha$  and non-compositional phase  $\gamma$ , the bias energy form for template  $m$  is

$$E^{(m)}(\mathbf{x}, \mathbf{z}) = F[D_1^{(m)}, \dots, D_6^{(m)}, \{G_T(\mathbf{x}, \mathbf{z})\}], \quad G_T(\mathbf{x}, \mathbf{z}) = \lambda_{x,2}G_T^\alpha + \frac{1}{2}\lambda_{z,2}G_T^\gamma \quad (14)$$

And the bias for ligand  $i$  is

$$e^{(i)}(\mathbf{x}, \mathbf{z}) = F[d_1^{(i)}, \dots, d_6^{(i)}, \{G_L(\mathbf{x}, \mathbf{z})\}], \quad G_L(\mathbf{x}, \mathbf{z}) = \lambda_{x,1}G_L^\alpha + \frac{1}{2}\lambda_{z,1}G_L^\gamma \quad (15)$$

These biases tend to exhibit a large gap between a few dominant templates and ligands and the rest. To ensure the participation of more ligands and templates in the strategy, we introduce cutoff energies for the ligand and template,  $e_c$  and  $E_c$ . We choose  $e_c$  to be the 21st lowest ligand energy and  $E_c$  to be the 4th lowest template energy. With this cutoff energy, the biased energy,  $e_b^{(i)}$ , for the  $i^{\text{th}}$  ligand becomes

$$e_b^{(i)}(\mathbf{x}, \mathbf{z}) = \begin{cases} e^{(i)}(\mathbf{x}, \mathbf{z}) & \text{if } e^{(i)} > e_c \\ e_c(\mathbf{x}, \mathbf{z}) & \text{otherwise} \end{cases} \quad (16)$$

And the biased energy,  $E_b^{(m)}$ , for the  $m^{\text{th}}$  template become

$$E_b^{(m)}(\mathbf{x}, \mathbf{z}) = \begin{cases} E^{(m)}(\mathbf{x}, \mathbf{z}) & \text{if } E^{(m)} > E_c \\ E_c(\mathbf{x}, \mathbf{z}) & \text{otherwise} \end{cases} \quad (17)$$

In one Monte Carlo move, if the  $i^{\text{th}}$  ligand in the molecule is to be changed at new zeolite values  $\mathbf{x}'$  and  $\mathbf{z}'$ , the biased probability for selecting another ligand  $l'_i$  from the ligand library is

$$f[E(\mathbf{n})] = \frac{\exp[-\beta e_b^{(l'_i)}(\mathbf{x}', \mathbf{z}')] }{\sum_{j=1}^{N_L} \exp[-\beta e_b^{(j)}(\mathbf{x}', \mathbf{z}')] } \quad (18)$$

For reverse move, we have

$$f[E(\text{o})] = \frac{\exp[-\beta e_{\text{b}}^{(l_i)}(\mathbf{x}, \mathbf{z})]}{\sum_{j=1}^{N_{\text{L}}} \exp[-\beta e_{\text{b}}^{(j)}(\mathbf{x}, \mathbf{z})]} \quad (19)$$

Similarly, if the template is desired to be changed at new zeolite values  $\mathbf{x}'$  and  $\mathbf{z}'$ , the biased probability for selecting template  $m'$  is

$$f[E(\text{n})] = \frac{\exp[-\beta E_{\text{b}}^{(m')}(\mathbf{x}', \mathbf{z}')] }{\sum_{j=1}^{N_{\text{T}}} \exp[-\beta E_{\text{b}}^{(j)}(\mathbf{x}', \mathbf{z}')] } \quad (20)$$

For reverse move, we have

$$f[E(\text{o})] = \frac{\exp[-\beta E_{\text{b}}^{(m)}(\mathbf{x}, \mathbf{z})]}{\sum_{j=1}^{N_{\text{T}}} \exp[-\beta E_{\text{b}}^{(j)}(\mathbf{x}, \mathbf{z})]} \quad (21)$$

To satisfy the detail balance, the acceptance rule becomes

$$\text{acc}(\text{o} \rightarrow \text{n}) = \min \left\{ 1, \frac{f[E(\text{o})]}{f[E(\text{n})]} \exp(-\beta \Delta E) \right\} \quad (22)$$

Parallel tempering is known to be a powerful tool for searching rugged energy landscapes [11, 12, 13]. Parallel tempering can be combined with both Metropolis Monte Carlo and biased Monte Carlo. In parallel tempering, the samples are divided into  $k$  groups. The first group of samples is simulated at  $\beta_1$ , the second group is at  $\beta_2$ , and so on, with  $\beta_1 < \beta_2 < \dots < \beta_k$ . At the end of each round, samples in group  $i < k$  are allowed to exchange configurations with samples in group  $i + 1$  with probability  $p_{\text{ex}}$ . The acceptance

rule for a parallel tempering exchange move is

$$\text{acc}(o \rightarrow n) = \min[1, \exp(\Delta\beta \Delta E)] \tag{23}$$

where  $\Delta\beta = \beta_i - \beta_{i+1}$  and  $\Delta E$  is the difference in energy between the sample in group  $i$  and the sample in group  $i + 1$  before the exchange is made. It is important to notice that this exchange step is experimentally cost-free. Nonetheless, this step can be dramatically effective at facilitating the protocol to escape from local minimum. The number of groups, the number of samples in each group, the value of  $\beta_i$ , and the exchange probability,  $p_{\text{ex}}$ , are experimental parameters to be tuned.

## 4 Results and Discussion

The size of the library is fixed at  $N_T = 15$  and  $N_L = 1000$ . We adjust  $\lambda_{x,i}$  and  $\lambda_{z,i}$  so that the synergistic terms will contribute on average as  $E_L : E_T : E_{LL} : E_{TL} = 1 : 1 : 2 : 1.2$  in the composition and non-composition phases. We also want a model in which the contribution from zeolite and molecule will be roughly of the same order for the optimal configurations obtained by grid or random protocols. Due to the complicated molecular terms, we find the parameters so that this occurs by trial and error. We first adjust all the  $\sigma_H$  values, then we adjust the  $\lambda_{x,i}$  and  $\lambda_{z,i}$  in eqs 6–9. As mentioned, we adjust the  $\lambda_{x,i}$  and  $\lambda_{z,i}$  so that the total molecular contribution from either type of phase accounts for roughly 15% of the corresponding constant phase term in  $E_{\text{zeolite}}$ .

To locate optimal parameters for the protocols, we perform a few short pre-experiments.

Since the size of the template library is relatively small, the optimal value for the probability of changing a template is  $p_{\text{template}} = 0.02$ . The maximum random displacements are  $|\Delta\mathbf{x}| = 0.1/\sqrt{d-1}$  and  $|\Delta\mathbf{z}| = 0.2$  in the composition space and non-composition space, respectively. For simple Metropolis Monte Carlo, the optimal inverse protocol temperature is  $\beta = 50$  for X3 and X4 and  $\beta = 20$  for X5. For the biased Monte Carlo schemes, the optimal inverse protocol temperature is  $\beta_b = 500$  for X3 and X4 and  $\beta_b = 200$  for X5. For biased Monte Carlo combined with parallel tempering, it is optimal to have the samples divided into three subsets, with 25% of the population at  $\beta_1 = \frac{1}{2}\beta_b$ , 50% at  $\beta_2 = \beta_b$ , and 25% at  $\beta_3 = 2\beta_b$ . The switching probability,  $p_{\text{ex}}$ , is 0.1. Determination of these parameter values corresponds experimentally to gaining familiarity with the protocol on a new system.

All the protocols are tested with increasing numbers of composition and non-composition variables. Results are shown in fig 2. From this figure, one can see that all multi-round Monte Carlo protocols are better than the single-pass protocols such as grid and random. The simple Metropolis method can find optimum samples that are twice as superior as those from the grid or random protocols. Most importantly, the biased Monte Carlo is especially efficient. The optimum sample energies from biased Monte Carlo far exceed the optimum sample energies from simple Metropolis with even 1000 rounds. Biased Monte Carlo is able to find such favorable samples mainly by finding much more favorable designs for the structure-directing agent. Parallel tempering is noticeably effective only for the more complicated X4 and X5 systems. For the relatively simple systems, such as X3, it is more important to keep all 1000 of the samples at the optimum temperature.

## 5 Conclusion

We have presented a model for high-throughput zeolite synthesis. As in previous studies, multi-pass Monte Carlo methods work better than do single-pass protocols. Sophisticated biased Monte Carlo schemes are highly efficient and much better than simple Metropolis Monte Carlo. Parallel tempering is the best method for complicated systems with 5 or more framework chemical compositional variables.

## Acknowledgment

It is a pleasure to acknowledge stimulating discussions with Daniel L. Cox that lead this work. This research was supported by the Alfred P. Sloan Foundation through a fellowship to M.W.D., the Chevron Research and Technology Corporation, and the National Science Foundation.

## Appendix: reflecting boundary conditions

The valid region of composition variables form a simplex, since they are non-negative and sum to unity. For those points near the corner of the allowed simplex, a high percentage of proposed moves will go beyond the allowed region. If those moves are simply rejected, the composition point will get stuck in the corner for a long time, and the limited sampling chances will be wasted. We want an algorithm that satisfies detail balance while avoiding getting stuck in the corners.

The scheme we have chosen ensures that all moves from any point in the simplex lead



to new valid points in the simplex. The scheme basically involves many reflections over the  $d - 2$  dimensional hyper-planes that define the boundaries of the simplex. Figure 3 shows how this works in the case of  $d = 3$  for a single reflection. We first define the unit normals,  $\mathbf{n}_i$ , to each of the faces of the simplex. We also find the constants  $c_i$  that define the faces by the equation  $\mathbf{x} \cdot \mathbf{n}_i = c_i$ . In the case of figure 3, there are three such unit normals and three such constants. We initially define  $\mathbf{y} = \mathbf{x}(o)$ . The algorithm consists of the following steps:

1. Test whether the proposed new point,  $\mathbf{x}$ , is in the allowed region. If so, define the new point  $\mathbf{x}(n)$  to be  $\mathbf{x}$  and stop.
2. If not, find the face  $i$  for which the quantity  $t_i = (c_i - \mathbf{y} \cdot \mathbf{n}_i) / [(\mathbf{x} - \mathbf{y}) \cdot \mathbf{n}_i]$  is minimal, taking into account only those faces for which both  $t_i$  and  $(\mathbf{x} - \mathbf{y}) \cdot \mathbf{n}_i$  are positive.
3. Define  $\mathbf{y} \leftarrow \mathbf{y} + t_i(\mathbf{x} - \mathbf{y})$ .
4. Reflect the point through this face by the equation  $\mathbf{x} \leftarrow \mathbf{x} - 2(\mathbf{x} \cdot \mathbf{n}_i - c_i)\mathbf{n}_i$ .
5. Continue with step 1.

This algorithm converges, because it decreases the magnitude of  $\mathbf{x}$  at each step, until  $\mathbf{x}$  is within the allowed region. The algorithm is also reversible. That is, for each forward move  $\mathbf{x}(o) \rightarrow \mathbf{x}$  that maps to the new position  $\mathbf{x}(n)$ , there is always a reverse move  $\mathbf{x}(n) \rightarrow \mathbf{x}'$  that maps to the original position  $\mathbf{x}(o)$ . Furthermore, when the original move is in the allowed move sphere,  $|\mathbf{x}(o) - \mathbf{x}| < \Delta x$ , the reverse move is as well,  $|\mathbf{x}(n) - \mathbf{x}'| < \Delta x$ . Given that we impose the detailed balance condition, then, these reflecting boundary conditions provide a valid Monte Carlo move from an old point in the allowed simplex to a new point in the allowed simplex.

These reflecting boundary conditions can be interpreted in a geometrical way. Essentially, the reflections perform a type of billiards in the  $d - 1$  dimensional simplex. In each attempted move, we chose a displacement  $\mathbf{x} - \mathbf{x}(o)$ . We can interpret the composition variable as a small ball that moves at a constant speed along this trajectory. The motion is continued until either a boundary is encountered or the entire length of the trajectory has been traveled. If a boundary of the simplex is encountered, the ball reflects off the hyper-plane by Newtonian mechanics, and the trajectory continues along the new, reflected direction. The motion, including possible additional reflections, is continued until the ball has traveled a distance equal to the chosen length of the displacement,  $|\mathbf{x} - \mathbf{x}(o)|$ . The location of the ball at the end of the trajectory then gives the new point  $\mathbf{x}(n)$ . The reverse move is given by exactly the reverse motion, which has the same total displacement.

## References

- [1] ZONES, S. I., NAKAGAWA, Y., LEE, G. S., CHEN, C. Y., and YUEN, L. T., 1998, *Micro. Meso. Mater.*, **21**, 199.
- [2] DAVIS, M. E., and ZONES, S. I., 1997, in *Synthesis of Porous Materials: Zeolites, Clays, and Nanostructures*, edited by OCCELLI, M. L., and KESSLER, H., pp. 1–34 (New York: Marcel Dekker).
- [3] BURKETT, S. L., and DAVIS, M. E., 1995, *Chem. Mater.*, **7**, 920.
- [4] BURKETT, S. L., and DAVIS, M. E., 1995, *Chem. Mater.*, **7**, 1453.
- [5] FALCIONI, M., and DEEM, M. W., 2000, *Phys. Rev. E*, **61**, 5948.

- [6] DEEM, M. W., 2001, in *Advances in Chemical Engineering*, edited by CHAKRABORTY, A., volume 28, pp. 81–121 (San Diego: Academic Press).
- [7] CHEN, L., and DEEM, M. W., 2001, *J. Chem. Inf. Comput. Sci.*, **41**, 950.
- [8] BRYNGELSON, J. D., and WOLYNES, P. G., 1989, *J. Phys. Chem.*, **93**, 6902.
- [9] SFATOS, C. D., and SHAKHNOVICH, E. I., 1997, *Phys. Rep.*, **288**, 77.
- [10] BOGARD, L. D., and DEEM, M. W., 1999, *Proc. Natl. Acad. Sci. U.S.A.*, **96**, 2591.
- [11] SWENDSEN, R. H., and WANG, J.-S., 1986, *Phys. Rev. Lett.*, **57**, 2607.
- [12] GEYER, C. J., 1991, in *Computing Science and Statistics: Proceedings of the 23rd Symposium on the Interface*, p. 156 (New York: American Statistical Association).
- [13] FALCIONI, M., and DEEM, M. W., 1999, *J. Chem. Phys.*, **110**, 1754.

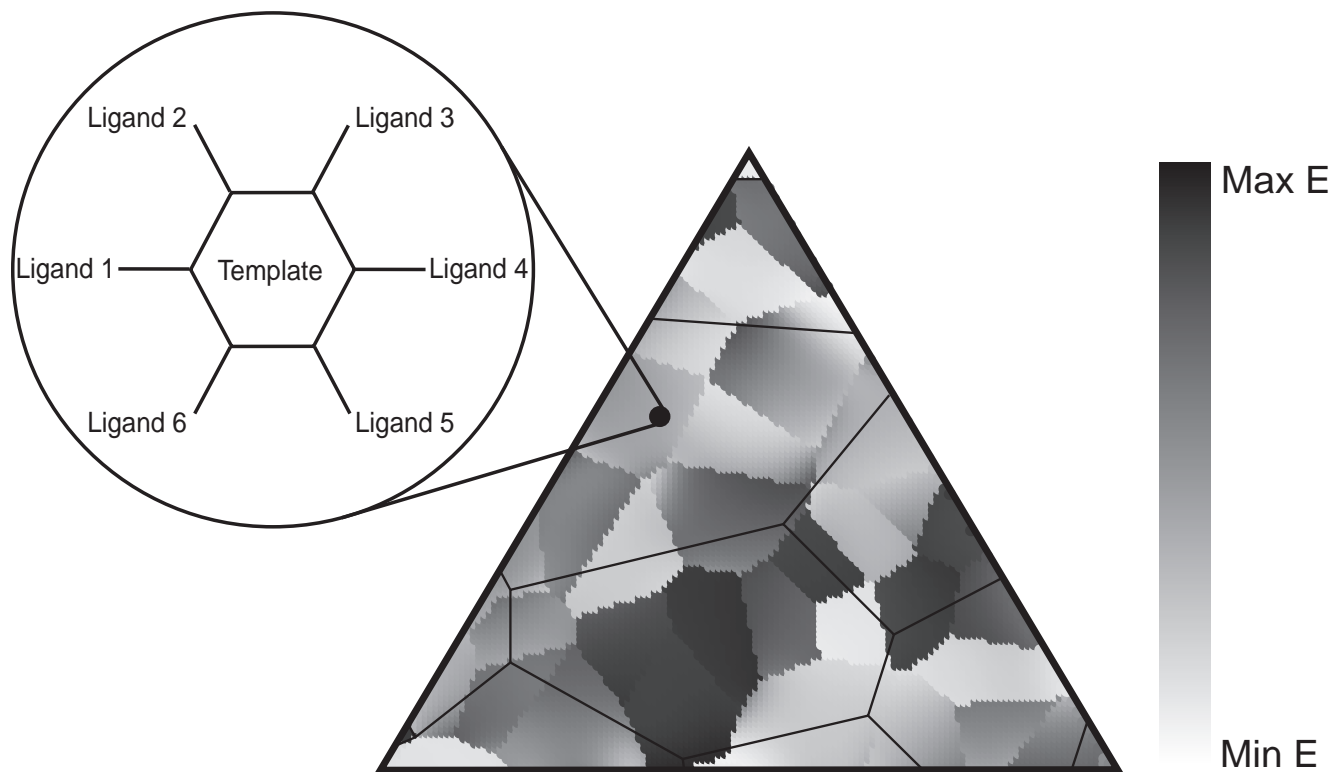


Figure 1: Schematic of the random energy model for templated zeolite synthesis.

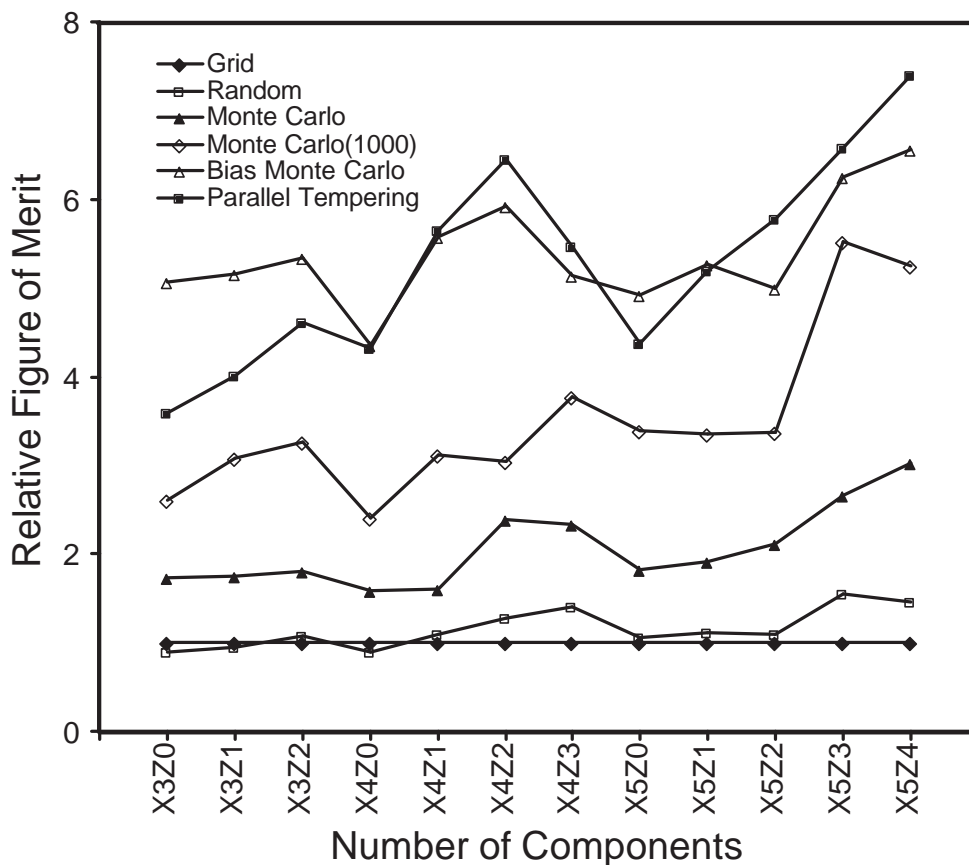


Figure 2: The minimum figure of merit found by different protocols with different number of composition ( $\mathbf{x}$ ) and non-composition ( $\mathbf{z}$ ) variables. The complexity of the structure-directing agent libraries is the same in all cases. The results are scaled to the minimum found by the grid searching method. Each value is averaged over scaled results on 10 different instances.

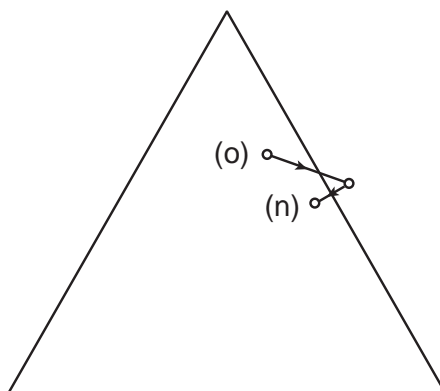


Figure 3: Schematic of the reflecting boundary conditions used to obtain valid composition variables.